# POST-BUCKLING ANALYSIS OF SLENDER ELASTIC RODS SUBJECTED TO TERMINAL FORCES AND SELF-WEIGHT

**M. A. Vaz**
Ocean Engineering Department, Federal University of Rio de Janeiro
P.O. Box 68508, 21945-970, Rio de Janeiro – RJ, Brazil

**G. H. W. Mascaro**
Ocean Engineering Department, Federal University of Rio de Janeiro
P.O. Box 68508, 21945-970, Rio de Janeiro – RJ, Brazil

Abstract. This article presents the behavior of slender elastic rods subjected to axial terminal forces and self-weight. The mathematical formulation is presented, a solution is sought for a double-hinged boundary condition and the analysis is carried out for different values of non-dimensional weight. The formulation derives from geometrical compatibility, equilibrium of forces and moments and constitutive relations yielding a set of six first order non-linear ordinary differential equations with boundary conditions specified at both ends, which characterizes a complex two-point boundary value problem. Furthermore, a perturbation method is used to find the critical buckling loads and initial post-buckling solutions. A numerical integration scheme based on a three parameter shooting method is employed in the post-buckling solutions.

Keywords: Buckling, Post-Buckling, Initial Post-Buckling, Instability.

## 1. INTRODUCTION

A large number of papers have been published on buckling and post-buckling of slender rods since Bernoulli, Euler and Lagrange's classical analytical contributions in the 18th century. An excellent review of the early developments in this field is presented by Love (1944). This class of problem exhibits several interesting phenomena, as described in previous research, such as limit load, bifurcation, jump and hysteresis.

There has certainly been more work published on weightless rods. Gurfinkel (1965) calculated the critical buckling loads for elastically restrained rods. Wang (1997) presented formulation and solution for large displacement configurations of clamped-hinged rods. Tan and Witz (1995) developed analytical solution for elastic rods subjected to terminal forces and moments. Lee and Oh (2000) provided a solution for the Bernouilli-Euler beam with variable cross-section and constant volume. Vaz and Silva (2002) developed a solution for rod post-buckling with boundary conditions hinged and elastically restrained.

Several models have also been studied for buckling and initial post-buckling of rods subjected to variable axial forces, mainly motivated by the use of long submersed rods such as marine risers and drill-strings in the offshore oil&gas exploitation. Lubinski (1950) employed a power series solution to calculate buckling loads of vertical drill-strings. Huang and Dareing (1966, 1968 and 1969), Plunkett (1967), Wang (1983), Bernitsas and Kokkinis (1983a-b and 1984), Vaz and Patel (1995) and Patel and Vaz (1996) also researched the rod buckling and initial post-buckling characteristics employing power series or Galerkin solutions. However, the problem of post-buckling of slender elastic vertical rods subjected to self-weight is not adequately addressed in literature. Recently Jurjo et al (2001) partially provided numerical and experimental results for large deflections of slender bars under self-weight.

## 2. MATHEMATICAL FORMULATION OF THE PROBLEM

The mathematical formulation derives from considering geometrical compatibility, equilibrium of forces and moments and constitutive relations. Hence a system of six first order non-linear ordinary differential equations is set to describe the elastica of deflected rods subjected to an axial variable load due to its self-weight, as shown in Figure 1a.

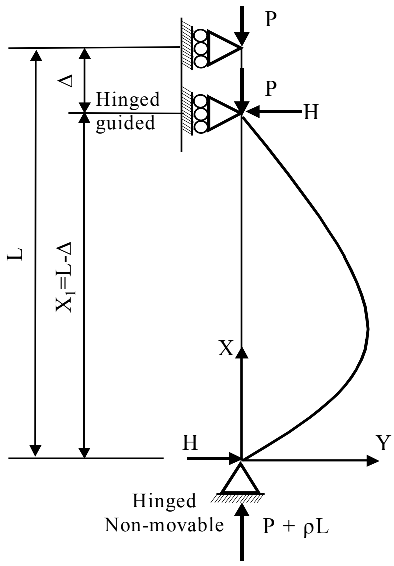


Figure 1a - Schematic of a Deflected Vertical Rod Subjected to Self-Weight.

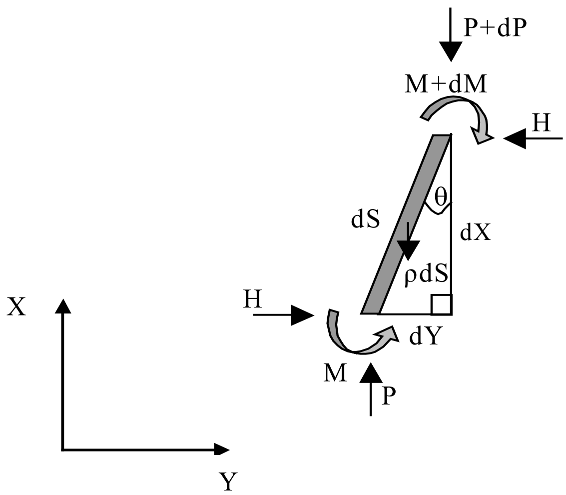


Figure 1b – Infinitesimal Element of Rod.

**Geometrical Compatibility**

Applying trigonometrical relations to the infinitesimal rod element $dS$ (see figure 1b) yields:

$$\frac{dX}{dS} = \cos\theta \tag{1a}$$

$$\frac{dY}{dS} = sin\theta \tag{1b}$$

Where $S$ is the rod arc-length ($0 \le S \le L$), $(X,Y)$ are the Cartesian coordinates of the deflected rod and $\theta$ is the angle between the tangent and the $X$-axis. Furthermore the curvature $\mathrm{K}$ is given by:

$$\mathrm{K} = \frac{d\theta}{dS} \tag{1c}$$

**Equilibrium of Forces and Moments**

A schematic of the internal forces and moments in the rod infinitesimal element is shown in figure 1b. The equilibrium of vertical and horizontal forces and bending moments, respectively yield:

$$\frac{dP}{dS} = -\rho \tag{2a}$$

$$\frac{dH}{dS} = 0 \tag{2b}$$

$$\frac{dM}{dS} + P\,sin\theta - H\cos\theta = 0 \tag{2c}$$

Where $M$ is the bending moment, $H$ and $P$ are respectively the horizontal and vertical forces and $\rho$ is the distributed weight per unit length.

**Constitutive Relations**

Assuming linear elastic, homogeneous and isotropic materials, and considering the state of pure bending results in:

$$M = EI\,\mathrm{K} \tag{3}$$

Where $E$ is the modulus of Young and $I$ is the cross-sectional second moment of inertia.

Therefore, substituting equation (3) into (2c) results:

$$EI\frac{d\mathrm{K}}{dS} = -P\,sin\theta + H\cos\theta \tag{4}$$

**Boundary Conditions**

A set of six boundary conditions must be defined and for the double-hinged rod they may be specified as:

$$X(0) = Y(0) = \mathrm{K}(0) = X(L) - X_1 = Y(L) = \mathrm{K}(L) = 0 \tag{5}$$

Where $X_1$ is the top end X-coordinate ( $X_1 = L - \Delta$ ). The effect of the boundary conditions on the rod buckling and post-buckling behavior is significant and it may be readily explored using the same methodology.

**The Governing Equations**

It is convenient to reduce the set of differential equations (1a), (1b), (1c), (2a), (2b) and (4) to a non-dimensional form using the following change of variables: $S = sL$, $Y = yL$, $X = xL$, $\mathrm{K} = \kappa/L$, $\rho = \overline{\rho}\,EI/L^3$ , $P = p\,EI/L^2$ and $H = h\,EI/L^2$ , where $0 \le s \le 1$. Hence:

$$\frac{dx}{ds} = \cos\theta \tag{6a}$$

$$\frac{dy}{ds} = sin\theta \tag{6b}$$

$$\frac{d\theta}{ds} = \kappa \tag{6c}$$

$$\frac{dp}{ds} = -\overline{\rho} \tag{6d}$$

$$\frac{dh}{ds} = 0 \tag{6e}$$

$$\frac{d\kappa}{ds} = -psin\theta + h\cos\theta \tag{6f}$$

Where $(x, y)$ constitute the deflected rod non-dimensional Cartesian coordinates, $s$ the non-dimensional arc-length, $\kappa$ the non-dimensional curvature, $\theta$ the angle formed by the curve tangent and the longitudinal axis, $p$ and $h$ respectively the non-dimensional longitudinal and lateral loads and $\overline{\rho}$ the non-dimensional weight.

Furthermore the boundary conditions given by equation (5) may be also made non-dimensional:

$$x(0) = y(0) = \kappa(0) = x(1) - x_1 = y(1) = \kappa(1) = 0 \tag{7}$$

Where $x_1 = 1 - \delta$ ($\delta = \Delta/L$). Equation (7) represents non-movable and movable (movement in the *x*-axis allowed) hinged conditions respectively at the lower and upper ends.

Buckling, initial post-buckling, and numerical integration solutions are sought for different values of $\overline{\rho}$.

## 3. THE INITIAL POST-BUCKLING SOLUTION

Poincaré's method - see Nayfeh (2000) - allows the solution to be written as an expansion in terms of a perturbation parameter $\varepsilon$ and perturbation coefficients $a_0, a_1, b_0, b_1$, rendering a set of sequentially, and analytically solvable, linear ordinary differential equations. Hence:

$$\theta(s) = \varepsilon\,\theta_0(s) + \varepsilon^3\,\theta_1(s) + \ldots \tag{8a}$$

$$h = \varepsilon\, b_0 + \varepsilon^3\, b_1 + \ldots \tag{8b}$$

$$p(0) = a_0 + \varepsilon^2\, a_1 + \ldots \tag{8c}$$

Where $\theta(s)$ and $h$ were expanded by odd functions whereas $p(0)$ was expanded by an even function because of the symmetrical nature of the problem. Note that $p(0)$ is the axial load at the lower end hence the load at the upper end is given by $p(1) = p(0) - \overline{\rho}$.

Integrating equation (6d) and using (8c) yields:

$$p(s) = (a_0 + \varepsilon^2\, a_1 + \ldots) - \overline{\rho}\, s \tag{8d}$$

When $\varepsilon = 0$ there is no perturbation and consequently no post-buckling, so $a_0$ is the non-dimensional critical buckling load at the lower end.

Expanding $\cos\theta$ and $sin\theta$ in Taylor series and using equation (8a) yields:

$$\cos\theta = 1 - \varepsilon^2\theta_0(s)^2 / 2! + \ldots \tag{9a}$$

$$sin\theta = \varepsilon\,\theta_0(s) + \varepsilon^3\left[\theta_1(s) - \theta_0(s)^3 / 3!\right] + \ldots \tag{9b}$$

Substituting equations (8a), (8b), (8d) into (6a)-(6f) and (7), expanding them and separating terms proportional to ε and $\varepsilon^3$ respectively yields:

$$\varepsilon \quad \begin{cases} \dfrac{d^2\theta_0(s)}{ds^2} + (a_0 - \overline{\rho}\, s)\,\theta_0(s) - b_0 = 0 \\[2ex] \dfrac{d\theta_0}{ds}(0) = 0 \\[2ex] \dfrac{d\theta_0}{ds}(1) = 0 \\[2ex] \displaystyle\int_0^1 \theta_0(s)\, ds = 0 \end{cases} \tag{10a}$$

$$\varepsilon^3 \quad \begin{cases} \dfrac{d^2\theta_1(s)}{ds^2} + (a_0 - \bar{\rho}\, s)\theta_1(s) - b_1 = (a_0 - \bar{\rho}\, s)\theta_0(s)^3/3! - b_0\,\theta_0(s)^2/2! - a_1\,\theta_0(s) \\ \dfrac{d\theta_1}{ds}(0) = 0 \\ \dfrac{d\theta_1}{ds}(1) = 0 \\ \displaystyle\int_0^1 \theta_1(s)ds = \frac{1}{3!}\int_0^1 \theta_0(s)^3\, ds \end{cases} \tag{10b}$$

The solution of the first order differential equation (10a) is sought by a power series function:

$$\theta_0(s) = \sum_{n=0}^{\infty} \mathrm{C}_\mathrm{n}\mathrm{s}^\mathrm{n} \tag{11a}$$

Which can be substituted in the differential equation (10a) and manipulated algebraically to give:

$$\begin{aligned} \theta_0(s) = C_0 + C_1\, s + \frac{1}{2}\left(-a_0 C_0 + b_0\right)s^2 + \frac{1}{6}\left(-a_0\, C_1 + \bar{\rho}\, C_0\right)s^3 + \\ + \frac{1}{12}\left[-\frac{1}{2}a_0\left(-a_0\, C_0 + b_0\right) + \bar{\rho}\, C_1\right]s^4 + \ldots \end{aligned} \tag{11b}$$

Applying the corresponding boundary conditions yields a homogeneous system of algebraic linear equations whose determinant is set to zero to avoid the trivial solution, and consequently the values of $a_0$ (buckling load), $C_0$ and $C_1$ may be found for a range of $\bar{\rho}$. For high values of $\bar{\rho}$ it is necessary to change the origin of the Cartesian axis system from the lower end to the neutral (zero tension) point of the rod to facilitate the computational processing.

Substituting $\theta_0(s)$ in the second order perturbation equation (10b) and again solving it by a power series function:

$$\theta_1(s) = \sum_{n=0}^{\infty} \mathrm{D}_\mathrm{n}\mathrm{s}^\mathrm{n} \tag{12a}$$

Substituting the equation (12a) in (10b), and after similar algebraic manipulation:

$$\begin{aligned} \theta_1(s) = D_0 + D_1\, s + \frac{1}{2}\left(-a_1\, C_0 - D_0\, a_0 + \frac{1}{6}a_0\, C_0{}^3 - \frac{1}{2}b_0\, C_0{}^2 + b_1\right)s^2 + \\ + \frac{1}{6}\left(-\frac{1}{6}\bar{\rho}\, C_0{}^3 + \frac{1}{2}a_0\, C_0{}^2\, C_1 - b_0\, C_0\, C_1 - a_1\, C_1 - D_1\, a_0 + D_0\, \bar{\rho}\right)s^3 + \\ + \frac{1}{12}\left(a_1\, a_0\, C_0 - \frac{1}{3}a_0{}^2\, C_0{}^3 + a_0\, C_0{}^2\, b_0 + D_1\, \bar{\rho} + \frac{1}{2}\left(D_0\, a_0{}^2 - \frac{1}{2}a_0\, b_1 - b_0\, C_1{}^2 - a_1\, b_0\right.\right. \\ \left.\left. - \bar{\rho}\, C_0{}^2\, C_1 - C_0\, b_0{}^2 + a_0\, C_0\, C_1{}^2\right)\right)s^4 + \ldots \end{aligned} \tag{12b}$$

The constant $b_0$ is set equal to $a_0$ and the boundary conditions must be applied in order to force the constants $D_0$ and $D_1$ to be zero because the homogeneous solution is already accounted for in the first order solution. A non-homogeneous system is then solved, the perturbation coefficients $a_1$ and $b_1$ are found, with results presented in figure 2. Once the perturbations coefficients are calculated, it is possible to determine the rod's geometrical configuration ( $x(s), y(s), \theta(s)$ ) for corresponding loads $p(s)$ (i.e., for any value of $\varepsilon$ ). Note that:

$$x(s) = s - \varepsilon^2/2!\int_0^s \theta_0(\xi)^2\, d\xi \qquad y(s) = \varepsilon\int_0^s \theta_0(\xi)d\xi + \varepsilon^3\int_0^s \left[\theta_1(\xi) - \theta_0(\xi)^3/3!\right]d\xi$$

$\kappa(s) = \varepsilon \ d\theta_0(s)/ds + \varepsilon^3 \ d\theta_1(s)/ds$ .

Furthermore, the axial top end displacement may be also obtained by $\delta = 1 - x(1)$ , or $\delta = \varepsilon^2 / 2! \int_0^1 \theta_0(s)^2 \, ds$ .

Important information can be withdrawn from the perturbation parameters, as a function of $\overline{\rho}$ , displayed in figure 2.

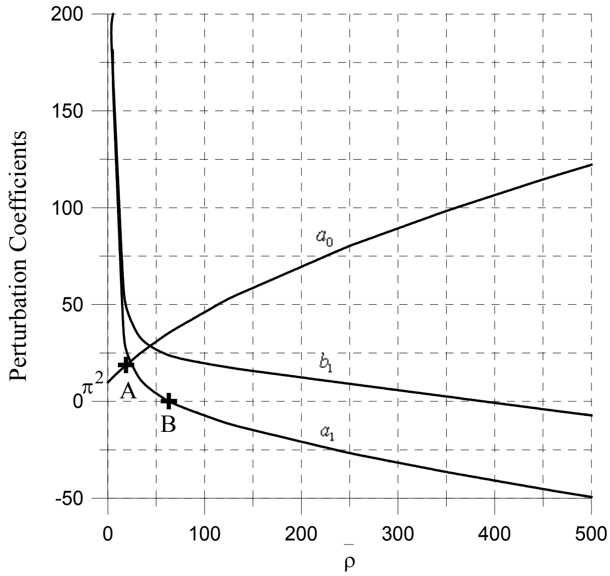


Figure 2 - Perturbation Coefficients as a Function of $\overline{\rho}$ .

When $\overline{\rho} = 0$ , there is no self-weight, so the critical buckling load $a_0$ is equal to $\pi^2$ as determined by Euler in 1744. For double-hinged weightless rods figure 2 shows that $a_1$ and $b_1$ tend to infinity, however, Vaz and Silva (2002) showed that a different perturbation scheme must be used since the horizontal force $h$ is zero. Hence:

$$p = \pi^2 + 1.2337\overline{\varepsilon}^2 + ...$$
$$\theta(s) = \overline{\varepsilon} \ \cos(\pi\, s) + \overline{\varepsilon}^3 \left[0.1964\, sin(\pi\, s) + 0.1654 \cos(\pi\, s) - 0.02083 \cos(3\pi\, s) - 0.1964\, s * sin(\pi\, s)\right] + ...$$

When the critical buckling load $a_0$ equals $\overline{\rho}$ (point *A* in figure 2), the axial force at the lower end $p(0)$ supports the entire rod weight and consequently the force at the upper end $p(1)$ equals zero. In other words, the rod buckles under its self-weight and no extra compressive force needs to be applied. This critical situation occurs for $\overline{\rho} = 18.5687$ .

If the lower end axial load $a_0$ is reached, the rod buckles as expected. Furthermore, the rod initial stability condition is determined by examining the perturbation coefficient $a_1$ . If $a_1$ is positive an increase in the load $p(0)$ (see equation (8c)) defines a stable post-buckling equilibrium configuration. However, if $a_1$ is negative, an axial force lower than $a_0$ (critical load) must be applied in order to be constituted a post-buckling configuration because $\varepsilon^2$ must be positive or null in equation (8c). A loss of stability is then experienced for values of $\overline{\rho} > 63.0675$ as $a_1$ becomes negative. The transition is indicated in figure 2 by point *B*.

The initial post-buckling solutions are also presented in figures 3a to 3d together with the full post-buckling mapping. It is shown that the buckling initiation process is well represented by the analytical solution.

## 4. THE POST-BUCKLING NUMERICAL SOLUTION

As the set of six first order non-linear ordinary differential equations and its boundary conditions specified at both ends characterize a two-point boundary value problem, a technique may be employed to transform it into an initial value problem and allow a direct integration scheme. Three boundary conditions are given at each end, see equation (7), so $h(0)$, $\theta(0)$ and $p(0)$ must be found. A shooting method available in Mathcad may be conveniently employed to compute the initial missing values. The following procedure is carried out: (a) the initial missing values are guessed;

(b) the boundary value endpoints are specified; (c) the set of differential equations is defined; (d) a load function which returns the initial condition is established; (e) a score function to measure the distance between terminal conditions and desired conditions is employed; (f) the equivalent initial conditions are finally calculated. From this point, a Runge-Kutta high order solution algorithm may be promptly applied to solve the set of non-linear differential equations.

Figures 3a to 3d respectively show the post-buckling and initial post-buckling curves $\delta \times h$, $\delta \times p(0)$, $\theta(0) \times h$ and $\theta(1) \times p(0)$ for $\overline{\rho} = 5, 63.0675, 125, 250, 350$. Figure 3a exhibits, as expected, symmetry. The maximum values of $h$ increase with $\overline{\rho}$ and the earlier the larger are the values of $\overline{\rho}$. When the upper end axial displacement is $\delta = 1$ the end points coincide, hence the loads at the lower and upper ends are respectively $\overline{\rho}/2$ and $-\overline{\rho}/2$ since $p(1) = p(0) - \overline{\rho}$. Figure 3b is anti-symmetric with respect to the line $\delta = 1$. For $\overline{\rho} < 63.0675$ the rod is initially stable as indicated by the positive curve slope. When $\overline{\rho} = 63.0675$ the rod buckles and "yields" at a constant load. When $\overline{\rho} > 63.0675$ an unstable region is encountered. If load is progressively applied the rod buckles (jumps!) before the critical load $p(0)$ is reached. If the process is displacement controlled the rod progressively deflects at reducing load. This phenomenon occurs in a narrower region for smaller values of $\overline{\rho}$, nonetheless the jump is more significant. Figures 3c and 3d show similar patterns when $0 \le \delta < 1$ and $1 < \delta \le 2$ respectively as the rod reverses its shape. As expected the rod angles $\theta(0)$ and $\theta(1)$ grow more rapidly when $\overline{\rho}$ increases.

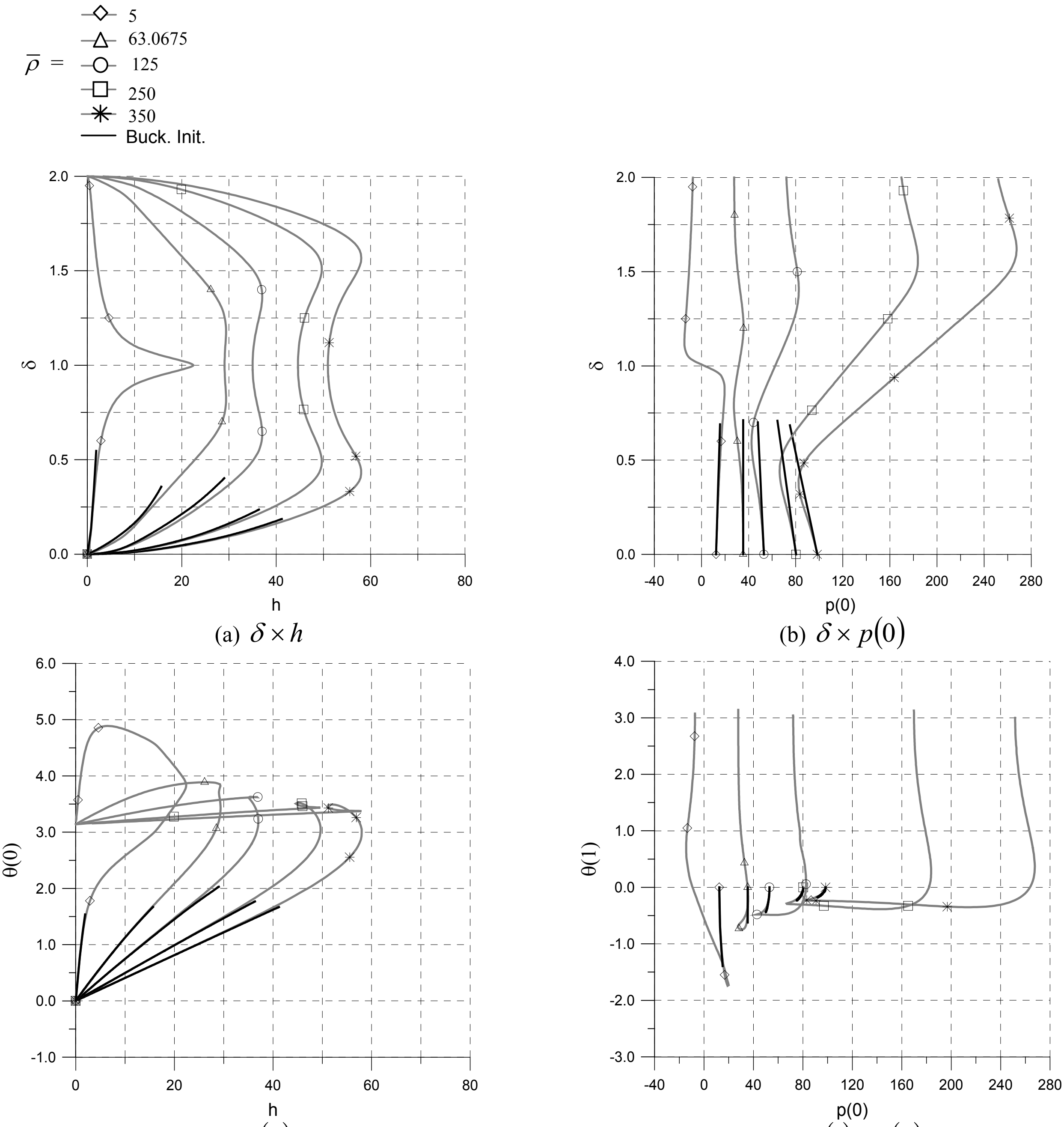


(a) $\delta \times h$

(b) $\delta \times p(0)$

(c) $\theta(0) \times h$

d) $\theta(1) \times p(0)$

Figure 3 - Post-Buckling Mapping

Figures 4a to 4f respectively present the post-buckling geometric configurations for $\overline{\rho} = 5, 35, 63.0675, 125, 250, 350$. In each graph the deformed shapes are displayed for $\delta = 0.1, 0.3, 0.5$ etc. The influence of the self-weight on the rod post-buckling behavior is evident. This effect becomes more asymmetric as $\overline{\rho}$ is progressively increased.

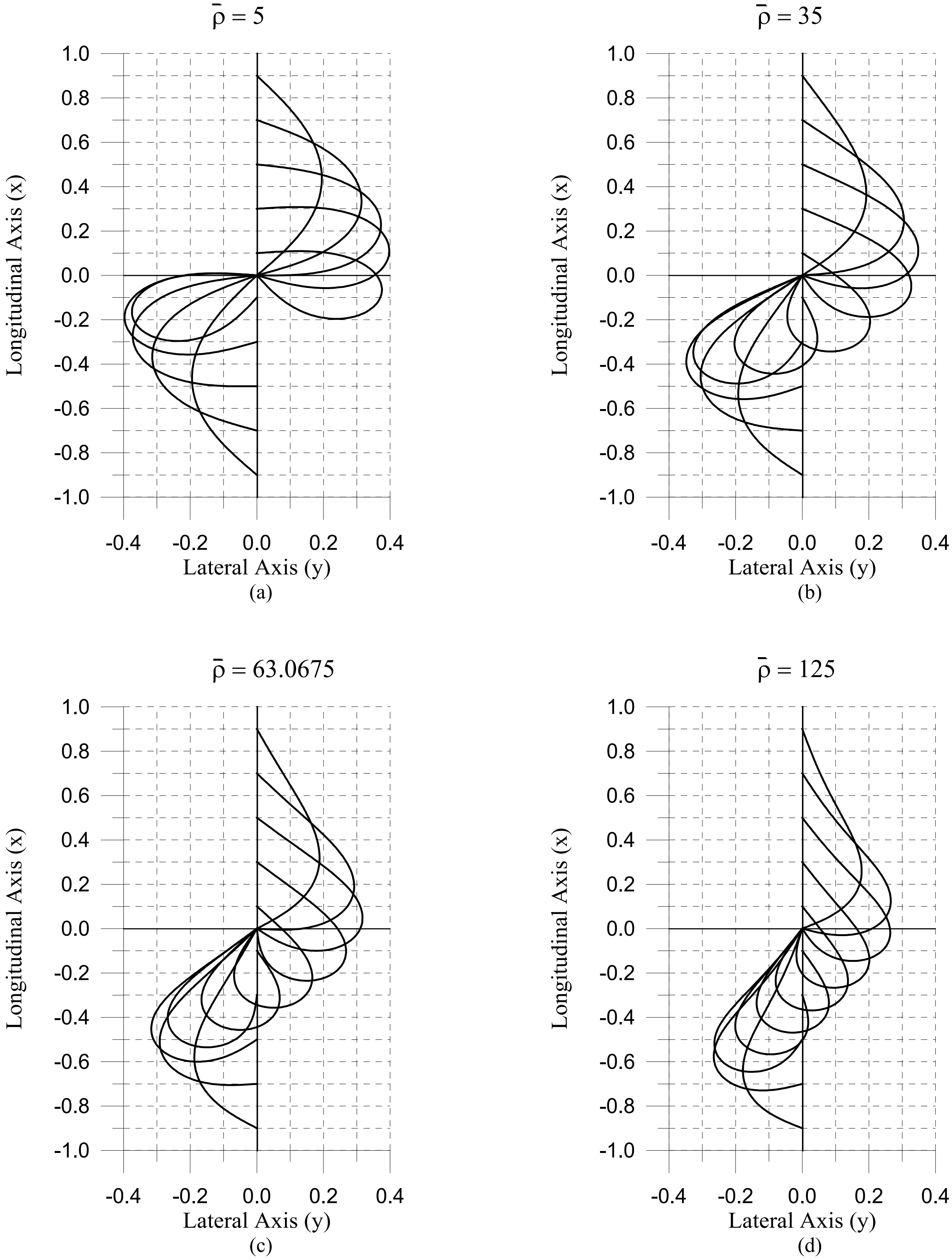


Figure 4 - Post-Buckling Geometric Configurations

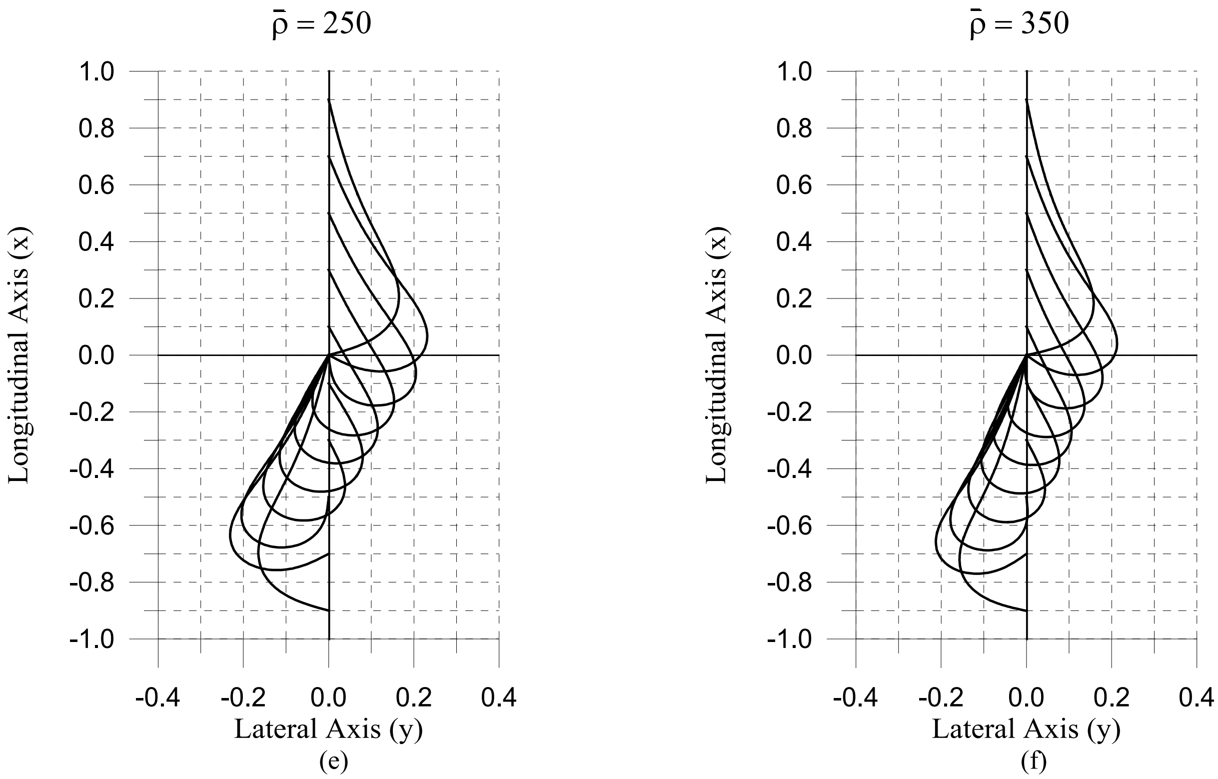


Figure 4 - Post-Buckling Geometric Configurations (continued)

## 5. CONCLUSIONS

This paper presents a formulation and a solution for the buckling and large deflection non-linear analysis of initially vertical elastic double-hinged rods subjected to terminal forces and a gravitational field. A perturbation scheme is developed to provide an analytical solution for the rod initial post-buckling. The rod post-buckling response is obtained from solving a complex two-point boundary value problem governed by a set of six first order non-linear ordinary differential equations. The numerical and analytical solutions developed in this paper are in sound agreement. The effect of the boundary conditions on the rod behavior is significant and it can be readily calculated with the methodologies developed.

The slender elastic rod stability behavior and its post-buckling configuration are greatly influenced by the value of the non-dimensional weight. The rod is shown to be initially stable up to a critical value of self-weight ( $\overline{\rho} < 63.0675$ for the non-dimensional parameterization employed) and unstable elsewhere.

## 6. ACKNOWLEDGEMENT

The authors acknowledge the support of the National Council for Scientific and Technological Development (CNPq) for this work.

## 7. REFERENCES


Bernitsas, M. M., Kokkinis, T.: Buckling of columns with nonmovable boundaries, J. Struct. Engineering **109**, 2113-2127 (1983).

Bernitsas, M. M., Kokkinis, T.: Buckling of columns with movable boundaries, J. Struct. Mechanics **11**, 351-370 (1983).

Bernitsas, M. M., Kokkinis, T.: Asymptotic behaviour of heavy columns and riser stability boundaries, ASME J. Appl. Mech. **51**, 560-565 (1984).

Gurfinkel, G.: Buckling of elastically restrained columns, ASCE J. Struct. Div. **91**, ST 6 159-183 (1965).

Huang, T., Dareing, D. W.: Predicting the stability of long vertical pipe transmitting torque in a viscous medium, J. Engineering for Industry, 191-200 (1966).

Huang, T., Dareing, D. W.: Buckling and lateral vibration of drill pipe, J. Engineering for Industry, 613-619 (1968).

Huang, T., Dareing, D. W.: Buckling and frequencies of long vertical pipes, J. Engineering Mechanics Division, Proceedings of the ASCE, Vol. 95, No. EM1, 167-181 (1969).

Jurjo, D. L. B. R., Gonçalves, P. B., Pamplona, D.: Large deflection behavior and stability of slender bars under self weight, Proceedings of the 16th Brazilian Congress of Mechanical Engineering, Uberlândia, Brazil, November 2001.

Lee, B. K., Oh, S. J.: Elastica and buckling load of simple tapered columns with constant volume. Int. J. Non-Linear Mech. **37**, 2507-2518 (2000).

Love, A. E. H.: A treatise on the mathematical theory of elasticity, 4th ed., New York: Dover Publications 1944.

Lubinski, A.: A study of the buckling of rotary drilling strings", API Drilling and Production Practice, 178-214 (1950).

MathCad: Mathcad 2000 Professional for PC, Mathsoft Inc. 2000.

Nayfeh, A. H.: Nonlinear interactions, 1st ed., New York: Wiley Interscience, 2000.

Patel, M. H., Vaz, M. A.: On the mechanics of submerged vertical slender structures subjected to varying axial tension, Proc. the R. Soc. London Ser. **A354**, 609-648 (1996).

Plunkett, R.: Static bending stresses in catenaries and drill strings, J. Engineering for Industry, 31-36 (1967).

Tan, Z., Witz, J. A.: On the deflected configuration of a slender elastic rod subject to parallel terminal forces and moments. Proc. R. Soc. London Ser. **A449**, 337-349 (1995).

Vaz, M. A., Patel, M. H.: Analysis of drill strings in vertical and deviated holes using the Galerkin technique, Engineering Structures **17**, 437-442 (1995).

Vaz, M. A., Silva, D. F. C.: Post-buckling analysis of slender elastic rods subjected to terminal force, Int. J. Non-Linear Mech. **34**, 483-492 (2002).

Wang, C. Y.: Post-buckling of a clamped-simply supported elastica. Int. J. Non-Linear Mech. **32**, 1115-1122 (1997).

Wang, C. Y.: Buckling and postbuckling of a long-hanging elastic column due to a bottom load. ASME J. Appl. Mech. **50**, 311-314 (1983).